Differential activity of pro-angiogenic CXC chemokines

Aigul Moldobaeva, **Amy Baek**, **Lindsey Eldridge**, and **Elizabeth M. Wagner**
Department of Medicine, Johns Hopkins University, Baltimore MD

Abstract

We showed previously in a mouse model of lung ischemia-induced angiogenesis, enhanced expression of the three ELR+ CXC chemokines (KC, LIX, and MIP-2) and that blockade of the ligand receptor $CXCR_2$ limited neovascularization. The present study was undertaken to determine the relative abundance and angiogenic potential of the three CXC chemokines and whether RhoA activation explained the measured differences in potencies. We found that LIX showed the greatest absolute amount in the in vivo model 4 hrs after left pulmonary artery obstruction (LIX>KC>MIP-2; $p<0.05$). In vitro, LIX induced the greatest degree of arterial endothelial cell chemotaxis and KC was without effect. A significant increase (~40%) in active RhoA was observed with both LIX and MIP-2 compared with vehicle control ($p<0.05$). On average, LIX induced the greatest amount of tube formation within pleural tissue in culture. Thus, the results of the present study suggest that among the three ELR+ CXC chemokines, LIX predominates in eliciting a pro-angiogenic phenotype.

INTRODUCTION

The chemokines are a family of proteins initially described to be important for recruiting leukocytes to sites of infection and inflammation. However, a subset of these cytokine proteins have been shown to be associated with blood vessel growth and repair (Keeley et al., 2008). Specifically, a growing body of evidence demonstrates the prevalence of the glutamic acidleucine-arginine (ELR+) CXC chemokines in the lung in association with neovascularization (Arenberg et al., 1998; Belperio et al., 2005; Strieter et al., 2003). In human tissue, the ELR+ chemokines have been shown to promote neovascularization through binding G-protein coupled receptors $CXCR_1$ and $CXCR_2$ and promoting systemic endothelial cell proliferation and migration (Li et al., 2003; Schraufstatter et al., 2001; Strieter et al., 1995). In mice, relatively little is known regarding the function of $CXCR_1$ since its expression was only recently confirmed (Fan et al., 2006; Fu et al., 2005; Moepps et al., 2006). The three ELR+ CXC chemokines that have been shown to function through the binding of $CXCR_2$ in mice are keratinocyte-derived chemokine (KC; CXCL1), lipopolysaccharide-induced chemokine (LIX; CXCL5), and macrophage inflammatory protein-2 (MIP-2; CXCL2). An explanation for this redundancy of protein expression or the unique contribution of each of these proteins to downstream signaling events leading to neovascularization has not been determined. However, after binding $CXCR_1/CXCR_2$, members of the Rho family of monomeric GTPases are activated and ultimately control endothelial cell chemotaxis (Schraufstatter et al., 2001).

Address all correspondence to: Elizabeth M. Wagner, Ph. D., Johns Hopkins Asthma and Allergy Center, Division of Pulmonary and Critical Care Medicine, 5501 Hopkins Bayview Circle, Baltimore, Maryland 21224, Telephone: 410-550-2506, FAX: 410-550-2612, wagnerem@jhmi.edu.

Differences in receptor binding capacity and second messenger activation also may exert selective responses among the chemokines and thereby lead to nuanced outcomes.

We have shown previously the importance of ELR+ CXC chemokines to neovascularization in a mouse model of lung ischemia-induced angiogenesis. An increase in mRNA expression of KC, LIX, and MIP-2 was observed early after ischemia (Srisuma et al., 2003). Increased MIP-2 protein was confirmed in lung homogenate by 4 hrs after the onset of ischemia and treatment with a neutralizing antibody to $CXCR_2$ limited systemic neovascularization of the lung (Sánchez et al., 2007). Furthermore, in an in vitro angiogenesis assay, we showed that activation of RhoA is critical for arterial endothelial cell chemotaxis induced by MIP-2 (Moldobaeva et al., 2008). Thus, the present study was undertaken to probe the differences in angiogenic potential of the three ELR+ CXC chemokines. Specifically, we assessed the relative abundance and angiogenic potencies of the three pro-angiogenic CXC chemokines and whether RhoA activation explained the measured differences in potencies.

METHODS

Lung chemokine proteins

Our in vivo protocol was approved by the Johns Hopkins Animal Care and Use Committee. Male mice (C57Bl/6, 5–6 weeks; Charles River Wilmington, MA) were studied as previously described (McClintock and Wagner, 2005; Wagner et al., 2008). Mice were anesthetized (2% isoflurane), intubated and ventilated (120 breaths/min, 0.2 ml/breath). After left lateral thoracotomy, the left pulmonary artery was ligated (LPAL) and the thoracotomy was closed while the mouse was placed on positive end-expiratory pressure (1 cmH$_2$O). The animal was removed from the ventilator, extubated and allowed to recover. For protein determination, anesthetized mice were sacrificed by cervical dislocation 4 hrs after left pulmonary artery ligation when the upper third of the left lung and the right lung were rapidly excised and frozen. We have shown previously that the upper left lung is pro-angiogenic whereas the lower left lung is not (Srisuma et al., 2003). Lung samples were weighed, homogenized (Polytron, Kinematica, Bohemia, NY) and aliquoted for protein determination. CXC chemokine proteins were determined by ELISA (Duoset Mouse MIP-2, LIX, and KC ELISA kits; R&D Systems, Minneapolis, MN) and normalized to total sample protein (BCA protein assay kit; Pierce, Rockford, IL).

Isolation of mouse aortic endothelial cells

As previously described, the aortas from C57Bl/6 mice (n=6) were dissected and placed with the intima side down on Matrigel-coated 35 mm tissue culture dishes (Moldobaeva and Wagner, 2005). After 4–6 days, endothelial cells that had migrated were replated to gelatinized T25 culture flasks and grown in supplemented DMEM (20% FCS, 15 µg/ml ECGS, 100 µg/ml penicillin/streptomycin, 0.25 µg/ml amphotericin B, and 0.1 mM MEM with non-essential amino acids). An endothelial cell phenotype was confirmed by immunostaining for PECAM, vWF, and uptake of Dil-ac-LDL. Only cells with positive staining were used for further experiments. All experiments were carried out using endothelial cells between passages 2–8.

Endothelial Cell Chemotaxis Assay

As previously described, polycarbonate filters (5 µm pore size, Corning Costar, Cambridge, MA) were coated with 0.2% gelatin, cells were detached (2 mM EDTA/PBS), washed and resuspended (DMEM with 0.1% fatty acid free BSA) (Moldobaeva et al., 2008) (Moldobaeva and Wagner, 2005). Endothelial cells (10^5) were added to the upper chamber of transwells (Corning Inc, Corning, NY) and incubated (37°C). After 1h, KC, LIX, or MIP-2 (0.1, 1.0 and 10 ng/ml; R&D Systems, Minneapolis, MN) was placed in the lower chamber and incubated for 2 hours. These concentrations were selected based on our previous work (Moldobaeva et

al., 2008; Moldobaeva and Wagner, 2005). Control conditions for all experiments were cells treated with vehicle (PBS) for a similar duration as agonist treatment. Non-migrated cells were removed and migrated cells were fixed and stained (Diff-Quik stain set; Dade Behring, Newark, DE). Membranes were mounted on slides and migrated cells were counted under a microscope (20x objective) in 5 fields across each membrane and averaged. Antibodies to $CXCR_1$ (rat-anti- human; $0.2\,\mu g/ml$) and $CXCR_2$ (mouse anti-human; $1\,\mu g/ml$) were used in the chemotaxis assay (Abcam, Cambridge, MA). Doses of antagonists were selected based on our previous experiments(Moldobaeva and Wagner, 2005).

Western Blot Analysis

Monolayer cells were stimulated and lysed in Laemmli buffer. Cell lysates were resolved by SDS-PAGE, transferred to nitrocellulose membrane, blocked (5% BSA in TBS-tween) and exposed to specific primary antibodies for each experiment. Total RhoA and Rac1 protein and RhoA and Rac1 activity were measured using kits from Upstate Biotechnology (Lake Placid, NY). RhoA and Rac1 activity were measured using rhotekin-RBD and PAK-1 PBD, respectively. These proteins possess binding domains that specifically pull down activated RhoA (Rho-GTP) and Rac1 (Rac1-GTP). After cells were treated and cell lysates were collected, Rho-GTP or Rac1-GTP were precipitated using rhotekin-RBD or PAK-1 PBD immobilized on agarose. Affinity precipitated RhoA, and Rac1 proteins as well as total RhoA and Rac1 were resolved by SDS-PAGE and detected by Western blotting. Each experiment was repeated in multiple different cell isolates. Immunoblots were quantified by densitometry using Un-Scan-It Gel software (Silk Scientific, Orem, UT) and compared to vehicle controls within the same membrane. RhoA and Rac1 activation were assessed 30 min after chemokine exposure.

Pleural tissue sprouting assay

Surface pieces of lung (1–2 mm) were placed in 96-well plates on 50 µl of Matrigel matrix growth factor reduced, covered with additional 50 µl of Matrigel and allowed to solidify in an incubator (37°C; 30 min). Subsequently, lung pieces were incubated for 7 days in media (DMEM, 20% FBS, antiobiotics-antimycotics) in the presence of vehicle or CXC chemokines (10 ng/ml; R&D Systems) which was replaced every other day. All experiments were conducted in triplicate. Cell sprouting was photographed in five fields/well with a 10x objective. Endothelial cell phenotype was confirmed in parallel experiments by staining with FITC-labelled anti-mouse CD31 antibody (BD Pharmingen, San Jose, CA). The lengths (µm) of the tubes of interconnecting cells were measured using Image Pro Plus 5.1 software (Media Cybernetics, Bethesda, MD). Measurements were made in a blinded manner by an individual unaware of the treatment protocol. Anti-RhoA, (Y-27632; 50 µM; Calbiochem, San Diego, CA) and Rac-1 inhibitor (5 µM; Calbiochem) were used to evaluate their importance for tube formation. Doses of antagonists were selected based on our previous work (Moldobaeva et al., 2008).

Statistics

All data are presented as the mean ± the standard error. Differences in chemokine responses were evaluated by 1-way ANOVA after log transforms of values. Group comparisons of statistically significant differences were made using Newman-Keuls test for multiple comparisons. A p value < 0.05 was accepted as a significant difference.

RESULTS

CXC chemokine protein

To determine the relative abundance of each of the three chemokine proteins early after left pulmonary artery ligation (LPAL) in vivo, we extracted lung tissue 4 hrs after LPAL. Figure 1 shows the significant increase in CXC chemokine protein expression normalized to total sample protein ($p<0.0001$). In absolute quantities, LIX was the most abundant of the three pro-angiogenic chemokines 4 hrs after LPAL followed by KC (LIX>KC; $p<0.05$) and MIP-2 was the least abundant (KC>MIP-2; $p<0.05$). For each chemokine, the left lung protein expression was significantly greater than right lung ($p<0.05$). A 2-4- fold increase in protein expression in the left upper lung compared to the right lung was observed for each of the chemokines and the average fold increase did not vary among the three chemokines (n=4 mice/chemokine).

Aortic Endothelial Cell Chemotaxis

Concentration-response relationships of mouse aortic endothelial cells to three doses of KC, LIX, and MIP-2 were obtained by counting migrated cell numbers. LIX appeared to promote the greatest number of cells to migrate (Figure 2; n=5 experiments). When basal chemotactic activity (vehicle) was subtracted from responses with increasing chemokine dose, only LIX showed a significant increase in the number of migrated cells at each dose ($p<0.05$). KC did not elicit significant responses at any dose and MIP-2 showed borderline significance ($p=0.06$) at the highest concentration. This analysis shows that LIX>MIP-2>KC with regard to chemotactic potential of aortic endothelial cells. Due to the lack of responsiveness of KC, studies to inhibit chemotaxis were limited to LIX and MIP-2 (10 ng/ml). Figure 3 shows the affects of anti-$CXCR_1$ and anti-$CXCR_2$ on chemokine - induced aortic cell migration. In this new series, both LIX and MIP-2 demonstrated a significant increase in the number of cells migrating in responses to chemokine stimulation (n=4; $p<0.05$). Since chemotaxis did not differ in response to the 2 chemokines, results were grouped to statistically assess the effects of pretreatment with antibodies to CXC receptors. Chemotaxis was significantly reduced after treatment with $CXCR_1$, $CXCR_2$, or the combination of $CXCR_1$ and $CXCR_2$ ($p<0.0001$) and the affects of these antibody treatments did not differ from each other.

RhoA and Rac1 activity

Since we previously showed that RhoA activation was essential for mouse aortic endothelial cell chemotaxis to MIP-2 (Moldobaeva et al., 2008) and others have shown the importance of both RhoA and Rac1 in the human arterial endothelial cell response to chemokine stimulation, we questioned whether there were differences in RhoA and Rac1 activation in response to KC, MIP-2 and LIX exposure. We measured active/total RhoA and Rac1 in aortic endothelial cells after exposure to each of the three chemokines (1ng/ml; n=5 experiments). Active RhoA under control conditions averaged 80% of total. A significant increase in RhoA was observed overall (Figure 4; $p=0.02$) with both LIX and MIP-2 showing a statistically significant increase (~40%) in activation compared with vehicle control ($p<0.05$). However, measurement of Rac1 activity showed no significant increase for any of the three chemokines (n=5 experiments). Active Rac1 under control conditions averaged 70% of total Rac1 protein.

Pleural tissue sprouting assay

An example of the effect of one of the CXC chemokines on tube formation in isolated lung tissue is shown in Figure 5. Note the left panel where endothelial cells are rounded and show no obvious pattern of assembly. The right panel shows tube-like structures (arrows) where endothelial cells align and extend in a sprouting pattern after exposure to LIX. The length of tubes was summed within each well and the average effects of the three CXC chemokines on the ability of pleural tissue to form tube-like structures in vitro are shown in Figure 6. Overall,

a significant increase in the summed tube lengths was observed when pleural lung tissue was treated with the chemokines (p<0.01) and lung tissue required these growth factors to induce tube formation. Staining samples with CD31 antibodies revealed that some, but not all cells of the tube-like structures, were endothelial cells. Yet, each of the three chemokines caused a significant increase in the length of tube elements compared to the vehicle control (p<0.01). Although not statistically different from each other due to considerable variability, average tube lengths/ field showed a rank order of LIX>KC>MIP-2. Furthermore, using inhibitors of RhoA and Rac1 had a significant effect on limiting tube formation within each chemokine treatment (p<0.01). Although somewhat variable for each chemokine, tube formation after treatment with either the RhoA inhibitor or the Rac1 inhibitor resulted in tube lengths not different from vehicle control levels. Thus, the chemokine-induced growth effect was almost completely inhibited by either RhoA or Rac1 inhibitors.

DISCUSSION

The ELR+ CXC chemokines have been shown to play a central role in response to tissue injury and repair. By their ability to promote leukocyte recruitment, predominantly polymorphonuclear cells, these chemokine proteins have been implicated in initiation and amplification of inflammatory diseases. However, evidence exists that many cell types besides inflammatory cells express chemokine receptors including endothelial cells (Chapman et al., 2009; Murdoch et al., 1999). Chemokines as mediators of neovascularization under conditions of malignancy, fibroproliferative disease, and wound repair have been described (Keeley et al., 2008). In the lung, we have shown that the ELR+ CXC chemokines play a critical role in promoting systemic neovascularization of the lung during pulmonary ischemia (Sánchez et al., 2007; Sukkar A et al., 2008). We have identified increased mRNA and protein of these chemokines in the lung tissue and have been able to substantially reduce the extent of neovascularization when using a CXCR2 neutralizing antibody in both mice (Sánchez et al, 2007) and rats (Sukkar et al, 2008). The present study was undertaken to probe the differences in angiogenic potential of the three ELR+ CXC chemokines in mice, KC (CXCL1), LIX (CXCL5), and MIP-2 (CXCL2). Specifically, we assessed the relative abundance and angiogenic potencies of these pro-angiogenic chemokines in several model systems. In summary, we found that LIX (CXCL5) protein showed the greatest absolute abundance in an in vivo mouse model, 4 hrs after left pulmonary artery obstruction. LIX also induced the greatest degree of arterial endothelial cell chemotaxis and along with MIP-2, showed substantial RhoA activation in cultured aortic endothelial cells. All three chemokines were effective at promoting tube formation within pleural tissue in culture. Thus, the results of the present study suggest that among the three ELR+ CXC chemokines, LIX and MIP-2 predominate in eliciting a pro-angiogenic phenotype.

Although originally described as predominantly macrophage-derived proteins, most inflammatory cells as well as lung structural cells have been shown to release CXC chemokines (Strieter and Kunkel, 1997). LIX has been shown to be expressed strongly by alveolar epithelial type II cells and fibroblasts but not by leukocytes challenged with LPS (Jeyaseelan et al., 2004; Smith and Herschman, 1995). Given our model of total left pulmonary artery ischemia, trapped blood-borne inflammatory cells as well as lung structural cells could contribute to the measured increases in in vivo protein expression. Although LIX showed the greatest absolute abundance, the increased expression relative to right lung controls was approximately equivalent (2-4-fold increase) for each of the three chemokines. However, with regard to providing a chemotactic gradient for thoracic vessels in contact with ischemic lung, absolute amount would be expected to be the most relevant parameter. We chose the 4 hr time point after LPAL since we showed previously an increase in the mRNA of each of the three CXC chemokines at this time (Srisuma, S., et al., 2003) and an increase in MIP-2 protein (Wagner, E. M., et al., 2008). However, it is possible that differences in magnitude may vary over the

time course of pulmonary ischemia. Future studies could discern whether a unique time course of release exists for these proteins.

To further define chemotactic potential, we studied isolated mouse arterial endothelial cells directly in culture. In this in vitro setting, we found KC to be without effect on arterial endothelial cell chemotaxis while LIX and MIP-2 induced significant migration of arterial endothelial cells. LIX was effective at a lower concentration yet maximum responses were equivalent to MIP-2 effects at the highest concentration studied (Figure 2 and Figure 3). Blockade of $CXCR_1$ and $CXCR_2$ provided approximately equivalent levels of inhibition of LIX- and MIP-2- induced chemotaxis suggesting overlapping affinities/receptor binding and/ or downstream signaling. These observations corroborate our previous results examining MIP-2-induced endothelial cell migration (Moldobaeva and Wagner, 2005). Interestingly, simultaneous application of both $CXCR_1$ and $CXCR_2$ antibodies suppressed chemotaxis completely. We studied mouse aortic endothelial cells as a surrogate to study angiogenic endothelial cell activity. We acknowledge however, endothelial cells recovered from actively growing vessels might show different responses.

Our previous work and that of others demonstrated that ELR^+ CXC chemokines mediate cytoskeletal changes within endothelial cells (Schraufstatter et al., 2001). Endothelial cell contraction and migration are mainly governed by endothelial cytoskeleton and adhesive membrane components. Schraufstatter and colleagues demonstrated in human endothelial cells, that chemokine-induced formation of actin stress fibers required RhoA activation. We confirmed in mouse endothelial cells the importance of RhoA activation for MIP-2 induced chemotaxis (Moldobaeva et al., 2008). Thus, in the present study we sought to evaluate the relative magnitude of RhoA activation with the three chemokines to determine whether differences in chemotaxis might be explained by RhoA activation. LIX and MIP-2 both resulted in consistent significant increases in RhoA that did not differ. Thus the two chemokines that showed similar maximal chemotaxis and effects of receptor blockade, also showed a similar increase in RhoA activation. As we showed previously (Moldobaeva et al., 2008), Rac1 activation appears not to be important for mouse endothelial cell chemotaxis under the experimental conditions studied.

In human lung pathology, it is the systemic circulation in the lung, the bronchial circulation, or sometimes other thoracic arteries of systemic origin that are pro-angiogenic. In the in vivo mouse model of angiogenesis after pulmonary ischemia, it is the systemic intercostal arteries that invade the ischemic lung and subsequently perfuse the lung (Mitzner et al., 2000). The pulmonary vasculature is not angiogenic and pulmonary artery endothelial cells do not respond to MIP-2 (Moldobaeva and Wagner, 2005). Furthermore, histologic examination of left lung sections at time points after the obstruction of the left pulmonary artery showed remarkable remodeling of the pleural surface in advance of the invasion of new vessels (Wagner et al., 2006). However, the depth of invasion of new systemic vessels and the site of anastomoses presumably with existing pulmonary capillaries is not known. Consequently, in the present study we questioned whether the chemokines released in the ischemic lung could promote de novo tube formation within the lung. We used Matrigel, a substrate used to examine endothelial cell tube formation, that has been widely used for in vitro measurement of angiogenesis. Interestingly, other cell types have been shown to have the potential to form tubes using this artificial matrix including fibroblasts, and some cancer cell lines (Staton et al., 2009). We studied normal lung tissue taken from the pleural surface, grown on Matrigel, and exposed it to each of the three chemokines separately. We found that each of the three chemokines could cause tube formation that did not differ significantly from each other, although LIX promoted the greatest average response. Interestingly, cultures stained with the endothelial cell surface marker CD31 demonstrated that some, but not all cells forming tubes, were endothelial cells. Although we have not characterized all the cells comprising the tube-like structures, others

have shown that a mixed population of endothelial cells, pericytes, fibroblasts, macrophages and dendritic cells can contribute. We conclude from these studies that, given the right environment with appropriate growth factors, pluripotent cells, presumably from lung pleura, can assemble into tube-like structures. Pleural tissue in Matrigel alone was without effect since only when chemokines were added did tube formation take place. Others have suggested that endothelial cells interact with surrounding matrix material and secrete proteases and plasminogen activators, resulting in basement membrane degradation, followed by migration into the surrounding matrix, proliferation and ultimately differentiation (Yokomori et al., 2009). These signals are integrated by the cell to regulate the complex changes in endothelial cell shape and motility required to form a network of endothelial tubes. The major determinant of cell motility and migration is actin activation and the Rho family of GTPases play a key role in regulating actin organization in the process of cell migration. Rac1 has been shown to trigger membrane ruffling and lamellopodia formation. Our results showed that RhoA and Rac1 activation were both essential for tube formation in this in vitro environment as RhoA and Rac1 blockade caused complete inhibition of tube formation.

In summary, we have shown that of the three ELR+ CXC chemokines, LIX and MIP-2 appear to induce systemic arterial endothelial cell chemotaxis equivalently and measurement of RhoA activation corroborates this finding. However, in the in vivo model, LIX expression is substantially greater than the other chemokines four hrs after left pulmonary artery ligation. We propose that LIX may provide the greatest stimulus in vivo for neovascularization after pulmonary ischemia.

Acknowledgments

REFERENCES

Arenberg DA, et al. Epithelial-neutrophil activating peptide (ENA-78) is an important angiogenic factor in non-small cell lung cancer. J Clin Invest 1998;102:465–472. [PubMed: 9691082]

Belperio JA, et al. Role of CXCR2/CXCR2 ligands in vascular remodeling during bronchiolitis obliterans syndrome. J Clin Invest 2005;115:1150–1162. [PubMed: 15864347]

Chapman RW, et al. CXCR2 antagonists for the treatment of pulmonary disease. Pharmacol Ther 2009;121:55–68. [PubMed: 19026683]

Fan X, et al. Murine CXCR1 is a functional receptor for GCP-2/CXCL6 AND IL-8/CXCL8. J Biol Chem. 2006

Fu W, et al. Cloning and characterization of mouse homolog of the CXC chemokine receptor CXCR1. Cytokine 2005;31:9–17. [PubMed: 15967374]

Jeyaseelan S, et al. Transcriptional profiling of lipopolysaccharide-induced acute lung injury. Infect Immun 2004;72:7247–7256. [PubMed: 15557650]

Keeley EC, et al. Chemokines as mediators of neovascularization. Arterioscler Thromb Vasc Biol 2008;28:1928–1936. [PubMed: 18757292]

Li A, et al. IL-8 directly enhanced endothelial cell survival, proliferation, and matrix metalloproteinases production and regulated angiogenesis. J Immunol 2003;170:3369–3376. [PubMed: 12626597]

McClintock JY, Wagner EM. Role of IL-6 in systemic angiogenesis of the lung. J Appl Physiol 2005;99:861–866. [PubMed: 15905327]

Mitzner W, et al. Angiogenesis in the mouse lung. Am J Pathol 2000;157:93–101. [PubMed: 10880380]

Moepps B, et al. A homolog of the human chemokine receptor CXCR1 is expressed in the mouse. Mol Immunol 2006;43:897–914. [PubMed: 16084593]

Moldobaeva A, et al. MIP-2 causes differential activation of RhoA in mouse aortic versus pulmonary artery endothelial cells. Microvasc Res 2008;75:53–58. [PubMed: 17662312]

Moldobaeva A, Wagner EM. Difference in Proangiogenic Potential of Systemic and Pulmonary Endothelium: Role of CXCR2. Am J Physiol Lung Cell Mol Physiol 2005:L1117–L1123. [PubMed: 15722378]

Murdoch C, et al. Cxc chemokine receptor expression on human endothelial cells. Cytokine 1999;11:704–712. [PubMed: 10479407]

Sánchez J, et al. The role of CXCR2 in systemic neovascularization of the mouse lung. J Appl Physiol 2007;103:594–599. [PubMed: 17556491]

Schraufstatter IU, et al. IL-8 activates endothelial cell CXCR1 and CXCR2 through Rho and Rac signaling pathways. Am J Physiol Lung Cell Mol Physiol 2001;280:L1094–L1103. [PubMed: 11350788]

Smith JB, Herschman HR. Glucocorticoid-attenuated response genes encode intercellular mediators, including a new C-X-C chemokine. J Biol Chem 1995;270:16756–16765. [PubMed: 7622488]

Srisuma S, et al. Identification of genes promoting angiogenesis in mouse lung by transcriptional profiling. Am J Respir Cell Mol Biol 2003;29:172–179. [PubMed: 12600816]

Staton CA, et al. A critical analysis of current in vitro and in vivo angiogenesis assays. Int J Exp Pathol 2009;90:195–221. [PubMed: 19563606]

Strieter, R.; Kunkel, SL. Chemokines. In: Crystal, RG., et al., editors. The Lung. Vol. Vol. 1. Philadelphia: Lippincott-Raven; 1997. p. 155-186.

Strieter RM, et al. CXC chemokines in vascular remodeling related to pulmonary fibrosis. Am J Respir Cell Mol Biol 2003;29:S67–S69. [PubMed: 14503558]

Strieter RM, et al. The functional role of the ELR motif in CXC chemokine-mediated angiogenesis. J Biol Chem 1995;270:27348–27357. [PubMed: 7592998]

Sukkar A, et al. Inhibition of CXCR2 Attenuates Bronchial Angiogenesis in the Ischemic Rat Lung. J Appl Physiol 2008;104:1470–1475. [PubMed: 18323463]

Wagner EM, et al. Pulmonary ischemia induces lung remodeling and angiogenesis. J Appl Physiol 2006;100:587–593. [PubMed: 16210444]

Wagner EM, et al. Inflammation and ischemia-induced lung angiogenesis. Am J Physiol Lung Cell Mol Physiol 2008;294:L351–L357. [PubMed: 18156440]

Yokomori H, et al. Caveolin-1 and Rac regulate endothelial capillary-like tubular formation and fenestral contraction in sinusoidal endothelial cells. Liver Int 2009;29:266–276. [PubMed: 19067793]
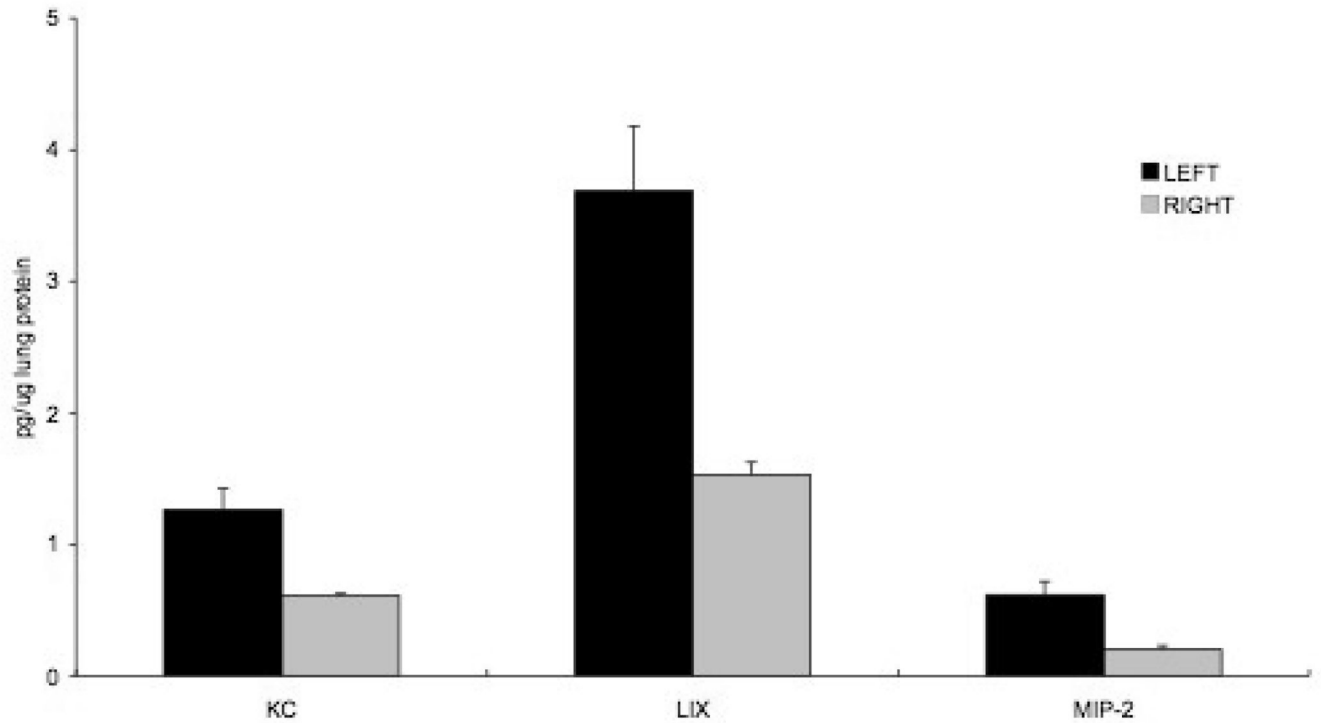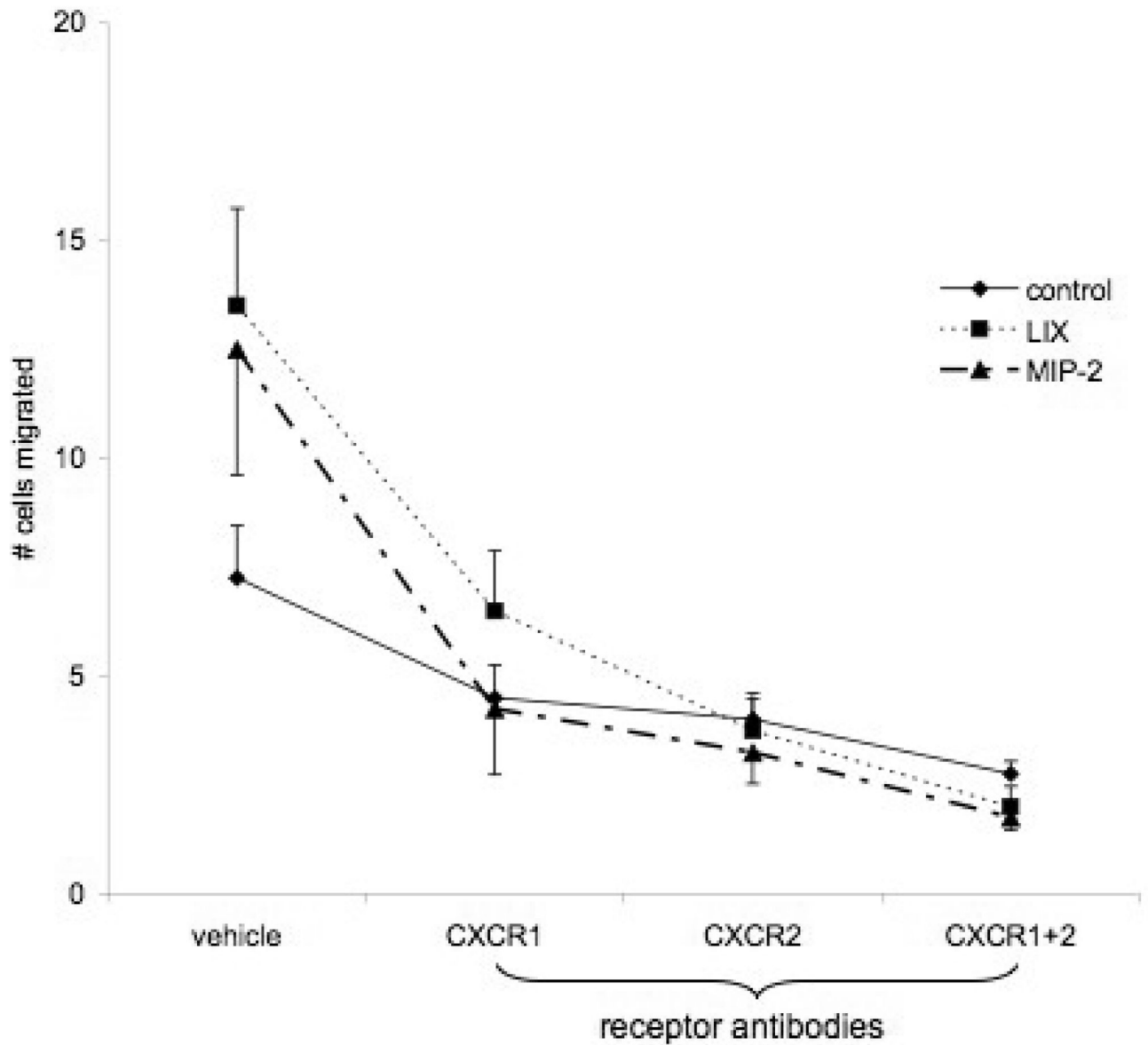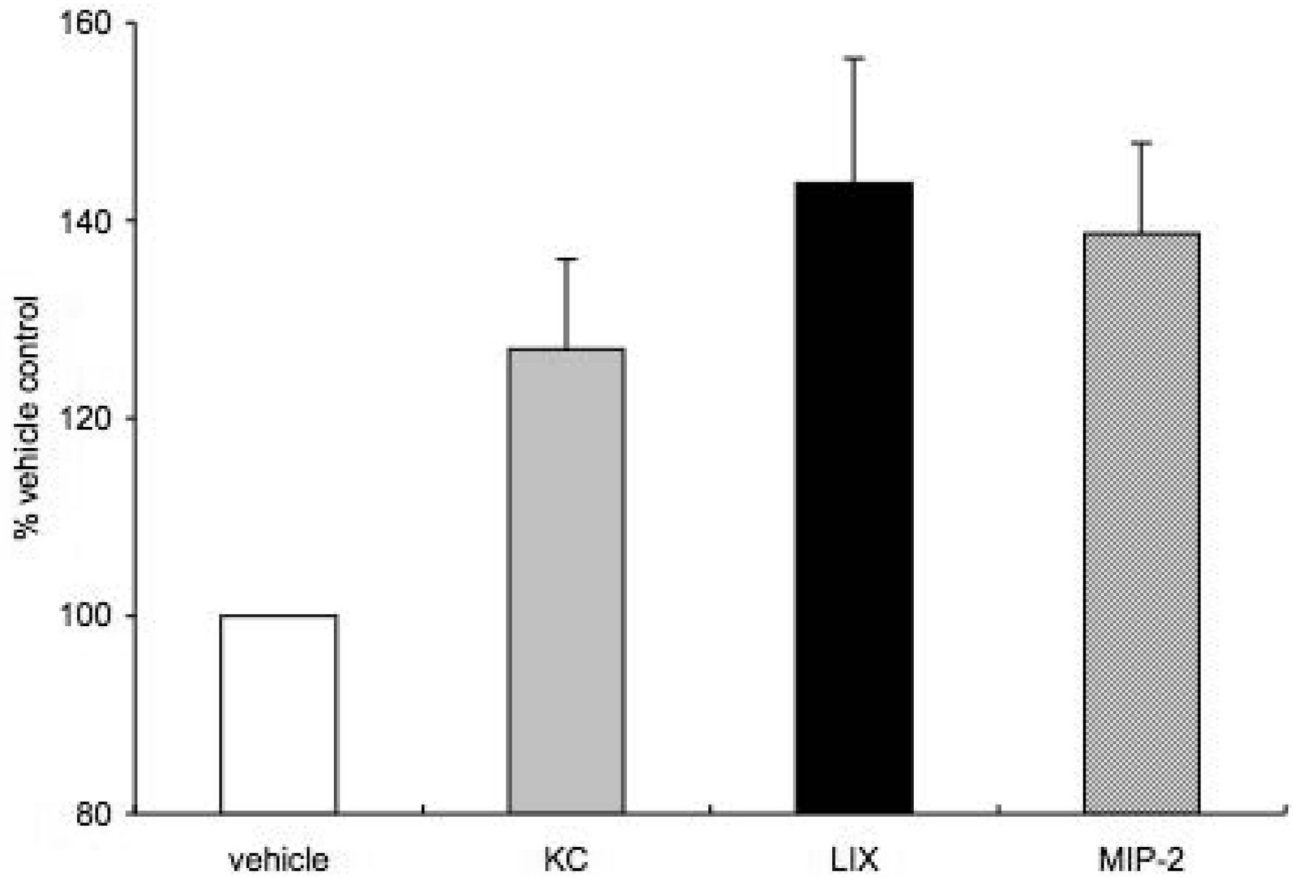
Figure 1.
CXC chemokine protein expression normalized to total sample protein in left and right lung homogenates 4 hrs after left pulmonary artery ligation (LPAL; p<0.0001). LIX was the most abundant followed by KC (LIX>KC; p<0.05) and MIP-2 was the least abundant (KC>MIP-2; p<0.05). For each chemokine, the left lung protein expression was significantly greater than right lung (p<0.05). The average 2-4 - fold increase did not vary among the three chemokines (n=4 mice/chemokine).
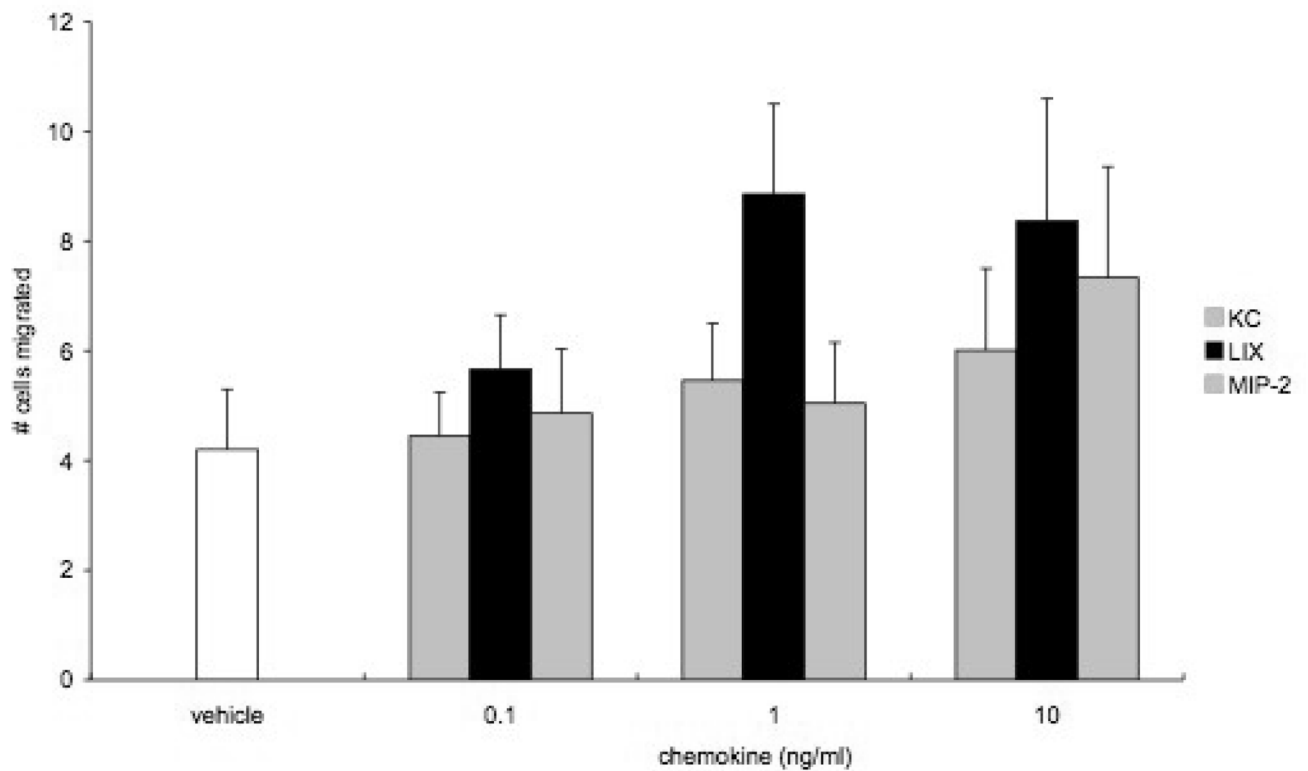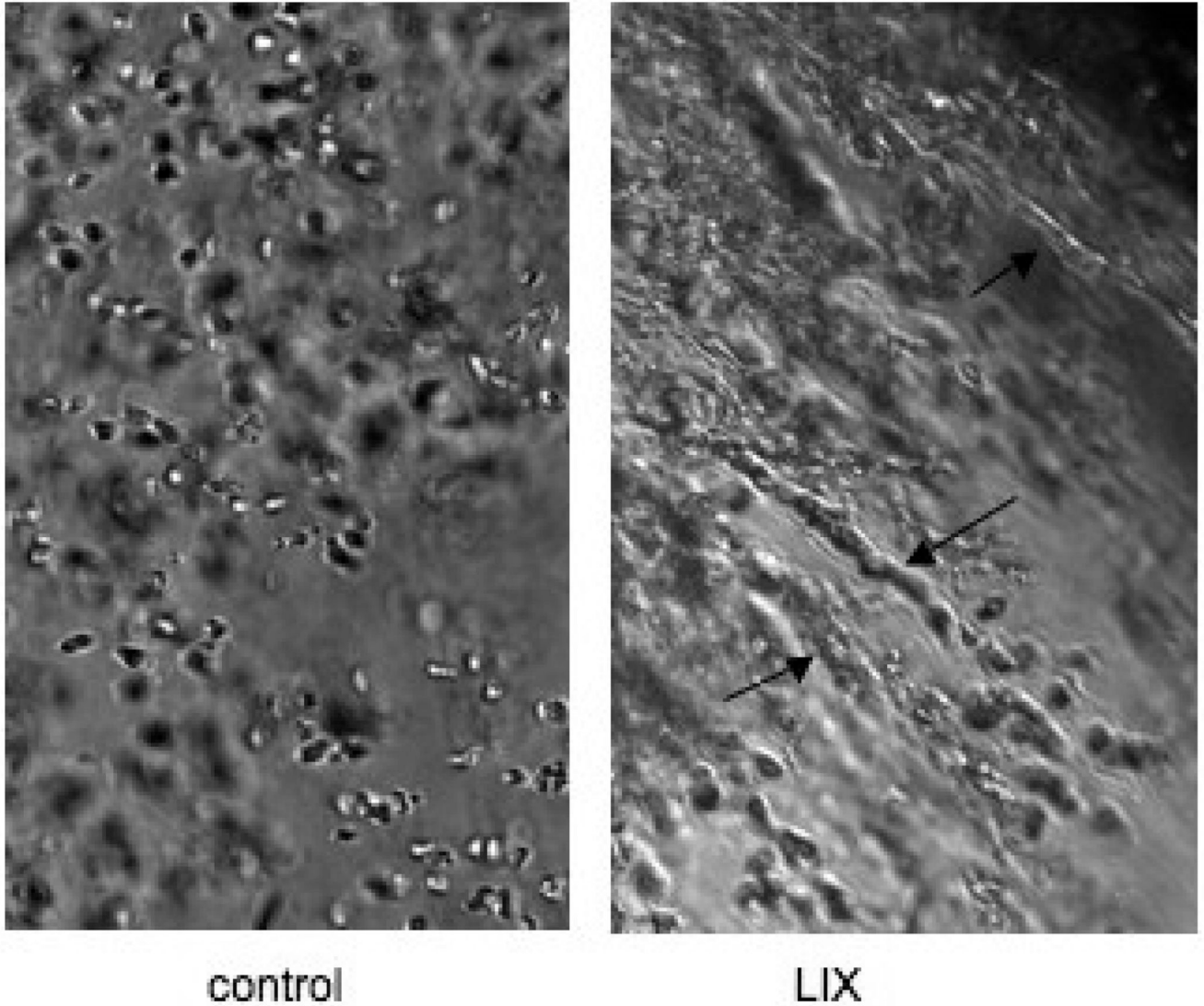
Figure 2.
Concentration-response relationships of mouse aortic endothelial cells to three doses of KC, LIX, and MIP-2 (n=5 experiments). Only LIX showed a significant increase in the number of migrated cells at each dose (p<0.05). KC did not elicit significant responses at any dose and MIP-2 showed borderline significance (p=0.06) at the highest concentration. This analysis shows that LIX>MIP-2>KC with regard to chemotactic potential of aortic endothelial cells.
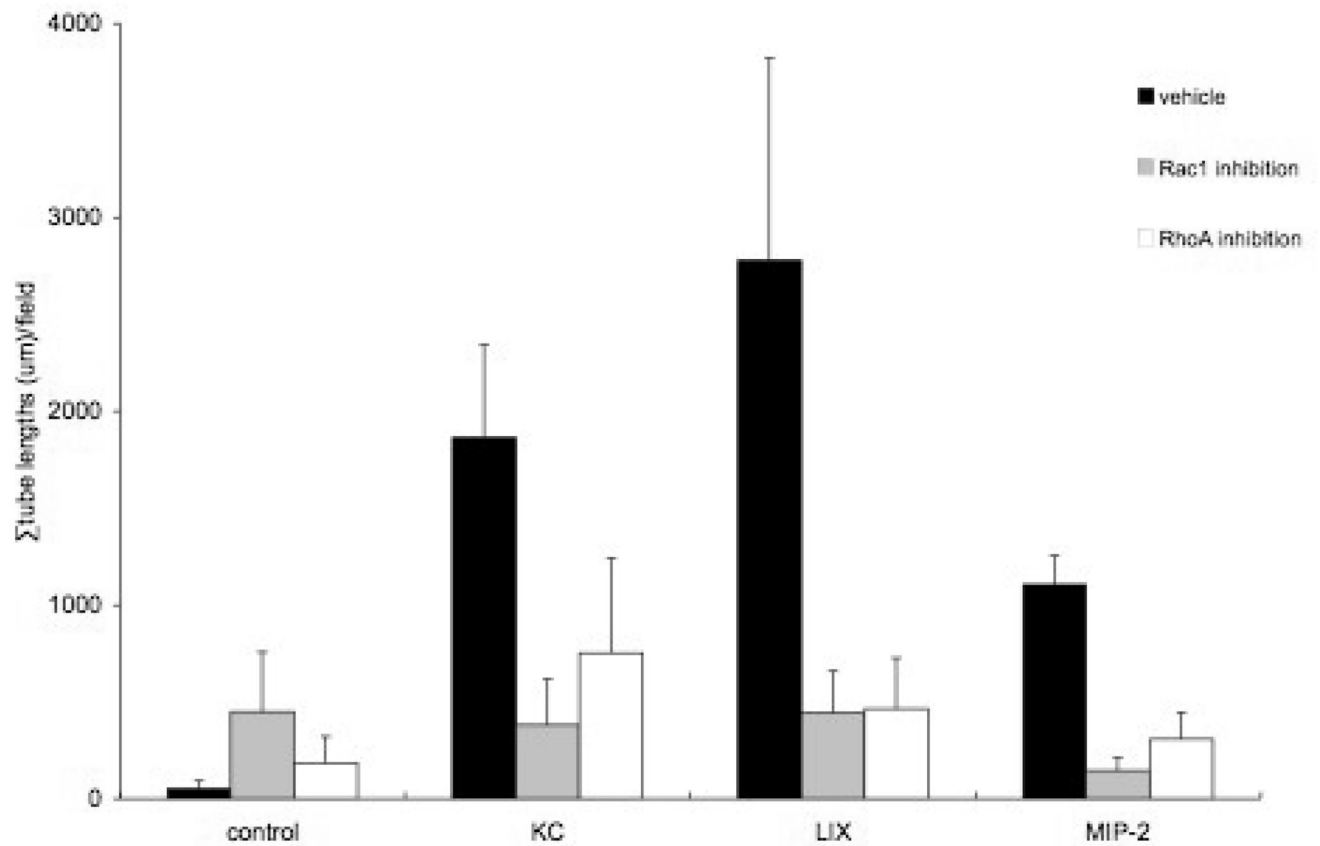
Figure 3.
Effects of anti-CXCR$_1$ and anti-CXCR$_2$ on chemokine - induced aortic cell migration.
Chemotaxis was significantly reduced after treatment with CXCR$_1$, CXCR$_2$, or the
combination of CXCR$_1$ and CXCR$_2$ (p<0.0001) and the affects of these antibody treatments
did not differ from each other.

Figure 4.
Active/total RhoA in aortic endothelial cells after exposure to each of the three chemokines
(n=5 experiments). Active RhoA under control conditions averaged 80% of total. A significant
increase (~40%) in active RhoA was observed with both LIX and MIP-2 compared with vehicle
control (p<0.05).

Figure 5.
Examples of tube formation in isolated lung tissue. The left panel (control) shows rounded endothelial cells and no obvious pattern of assembly. The right panel (LIX) shows tube-like structures (arrows) where endothelial cells align and extend in a sprouting pattern after exposure to LIX.

Figure 6.
Average effects of the three CXC chemokines on the ability of lung tissue to form tube-like structures in vitro. Each of the three chemokines caused a significant increase in the length of tube elements compared to the vehicle control (p<0.01). Average tube lengths/ field showed a rank order of LIX>KC>MIP-2. Within each chemokine treatment group, inhibitors of RhoA and Rac1 had a significant effect on limiting tube formation (p<0.01).